ANL/ET/CP--83023
CONF-950740--85

STATISTICAL ANALYSIS OF FATIGUE STRAIN-LIFE DATA FOR CARBON AND LOW-ALLOY STEELS*

J. Keisler† and O. K. Chopra
Energy Technology Division
†Decision and Information Sciences Division
Argonne National Laboratory
Argonne, IL 60439

March 1995

For presentation at the 1995 ASME/JSME Pressure Vessels and Piping Conference, July 23–27, 1995, Honolulu, HI.

*Work was supported by the Engineering Issues Branch, Office of Nuclear Regulatory Research (RES), U.S. Nuclear Regulatory Commission (NRC), under FIN Number W6077–3.

STATISTICAL ANALYSIS OF FATIGUE STRAIN–LIFE DATA FOR CARBON AND LOW–ALLOY STEELS

Jeffrey Keisler
Decision and Information Sciences Division
Argonne National Laboratory
Argonne, Illinois

Omesh K. Chopra
Energy Technology Division
Argonne National Laboratory
Argonne, Illinois

ABSTRACT

The existing fatigue strain vs. life (S–N) data, foreign and domestic, for carbon and low–alloy steels used in the construction of nuclear power plant components have been compiled and categorized according to material, loading, and environmental conditions. A statistical model has been developed for estimating the effects of the various test conditions on fatigue life. The results of a rigorous statistical analysis have been used to estimate the probability of initiating a fatigue crack. Data in the literature were reviewed to evaluate the effects of size, geometry, and surface finish of a component on its fatigue life. The fatigue S–N curves for components have been determined by applying design margins for size, geometry, and surface finish to crack initiation curves estimated from the model.

NOMENCLATURE

DO	Dissolved oxygen in water (ppm)
E	Young's modulus (GPa)
$F^{-1}[x]$	Inverse of the standard normal cumulative distribution function
I_S	Indicator for steel type. It is 1 for carbon steel and 0 for low–alloy steel.
I_W	Indicator for water environment. It is 1 for water and 0 for air environment.
N_{25}	Fatigue life defined as the number of cycles for peak tensile stress to drop 25% from its initial value
O^*	Transformed dissolved oxygen (ppm)
R	Strain ratio
R_a	Average surface roughness, defined as the arithmetic mean deviation of the surface height from the mean line through the profile
R_q	RMS surface roughness, defined as the root–mean–square deviation of the surface profile from the mean line
S	Sulfur content of the steel (wt.%)
S^*	Transformed sulfur content (wt.%)
S_a	Applied stress amplitude (MPa)
S_a'	Value of stress amplitude adjusted for mean stress (MPa)
T	Test temperature (°C)
T^*	Transformed temperature (°C)
X	Failure criteria defined as 25, 50, or 100% decrease in peak tensile stress
ε_a	Applied strain amplitude (%)
$\dot{\varepsilon}$	Applied total strain rate (%/s)
$\dot{\varepsilon}^*$	Transformed total strain rate
σ_u	Ultimate strength of the steel (MPa)
σ_y	Yield strength of the steel (MPa)

INTRODUCTION

The ASME Boiler and Pressure Vessel Code Section III, Subsection NB (1), contains rules for the construction of Class 1 components. Figure I–9.0 of Appendix I to Section III specifies the Code design fatigue curves that are to be used. However, Section III, Subsection NB–3121, of the Code states that environmental effects on fatigue resistance of a material are not explicitly addressed in these design curves. Therefore, there is uncertainty about the environmental effects on fatigue resistance of materials for operating pressurized water reactor (PWR) and boiling water reactor (BWR) plants, whose primary–coolant–pressure–boundary components are constructed as specified in Section III of the Code.

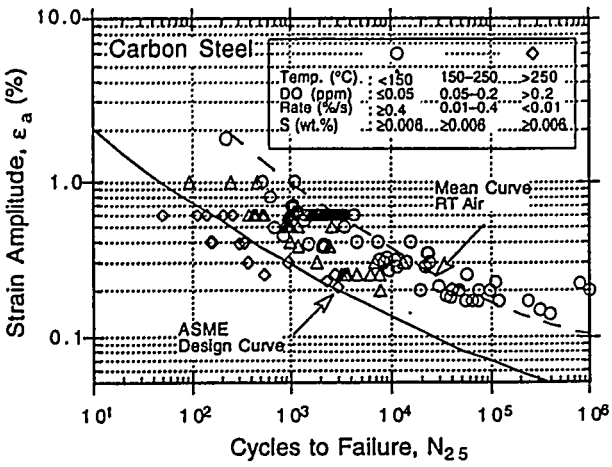

Figure 1. Fatigue S–N data for carbon steels in water

Current Section III design fatigue curves were based on strain–controlled tests of small polished specimens at room temperature (RT) in air (2). To obtain the design fatigue curves, best–fit curves to the experimental test data were lowered by a factor of 2 on stress or 20 on cycles, whichever was more conservative, at each point on the best–fit curve. As described in the Section III criteria document, these factors were intended to account for the differences and uncertainties in relating the fatigue lives of laboratory test specimens to those of actual reactor components. The factor of 20 on cycles is the product of three separate subfactors: 2 for scatter of data (minimum to mean), 2.5 for size effects, and 4 for surface finish, atmosphere, etc. (3). "Atmosphere" was intended to reflect the effects of an industrial environment rather than the controlled environment of a laboratory. The effects of the coolant environment are not explicitly addressed in the Code design curves. Furthermore, the probability distribution on fatigue life is not defined in the Code design fatigue curves. The best–fit or mean curves to the experimental data represent a 50% probability of initiating a fatigue crack in a small polished test specimen. It is not clear whether the Code design curve represents a 95, 50, or 5% probability of initiating a fatigue crack in power plant components.

Recent fatigue strain–vs.–life (S–N) data from the United States (4–14) and Japan (15,16) show that light water reactor (LWR) environments can have potentially significant effects on the fatigue resistance of carbon steel (CS) and low–alloy steel (LAS). Recent results on the effects of material and loading variables, e.g., steel type, strain rate, dissolved oxygen (DO), strain range, loading waveform, and surface morphology, on fatigue life of carbon and low–alloy steels are presented in a companion paper elsewhere in this proceedings. Fatigue lives in simulated LWR environments can be much shorter than the lives determined by corresponding tests in air, Fig. 1. Under certain conditions of loading and environment, e.g., temperature >250°C, DO >0.1 ppm, strain rate <0.01 %/s, and sulfur content in the steel ≥0.006 wt.%, fatigue lives in the test environments can be a factor of 100 shorter than those for the tests in air. This implies that the factors of 2 and 20 applied to the mean–data curve may not be adequate. Based on the existing fatigue S–N data, Argonne National Laboratory (ANL) has developed interim design fatigue curves that explicitly address environmental effects on fatigue life of CSs and LASs (17).

The objectives of this paper are to obtain the probability distribution on fatigue life of carbon and low–alloy steels and to quantify the contributions of various material, loading, and environmental conditions that influence the fatigue resistance of these steels. The statistical model and analysis presented in this paper are modified version of the results presented earlier in NUREG/CR–6237 (18). Existing fatigue S–N data, foreign and domestic, for CSs and LASs have been compiled and categorized according to different test conditions. A statistical model has been developed for estimating the effects of various material and service conditions on fatigue life. Results of the statistical analysis have been used to estimate the probability of initiating fatigue cracking. The contributions of material and environmental conditions that have not been considered in the existing fatigue S–N data base, such as size, geometry, and surface finish, are discussed.

OVERVIEW OF FATIGUE STRAIN–LIFE DATA

The primary sources of relevant S–N data are the tests performed by General Electric Co. (GE) in a test loop at the Dresden 1 reactor (4,5) and with the Electric Power Research Institute (EPRI) (6,7), the work of Terrell at Mechanical Engineering Associates (MEA) (8–10), the ongoing program at ANL on fatigue of pressure vessel and piping steels (11–14), and the JNUFAD[1] data base for "Fatigue Strength of Nuclear Plant Component" from Japan, including the work of Higuchi, Kobayashi, and Iida (15,16). In addition, fatigue tests have been conducted by Babcock and Wilcox (B&W) in water chemistries that are characteristic of fossil–fired boilers (19). Although the B&W data exhibit trends similar to those observed in LWR environments, the B&W data were not considered in this study.

Only fatigue data obtained on smooth specimens tested under fully reversed loading conditions were considered in this analysis; tests on notched specimens or at R values other than –1 were excluded. Details of the fatigue data from different sources are given in Table 1. The data base is composed of 456 tests in air (345 tests for LAS and 111 for CS) and 409 tests in water (270 tests for LAS and 139 for CS). Carbon steels include nine different heats of A333–Grade 6, A106–Grade B, A516–Grade 70, and A508–Class 1 steel, while the low–alloy steels include 14 heats of A533–Grade B and A508–Class 2 and 3 steel. Most of the data have been obtained on cylindrical specimens tested under axial strain–control mode using a triangle or sawtooth waveform. The specimen diameters range from 6 to 10 mm and gauge lengths range from 8 to 25 mm (tests conducted on

[1]Private communication from M. Higuchi, Ishikawajima–Harima Heavy Industries Co., Japan, to M. Prager of the Pressure Vessel Research Council, 1992. The old data base "FADAL" has been revised and renamed "JNUFAD."

Table 1. Data base for fatigue S–N behavior of carbon and low–alloy steels

Source	Reference	Steel Type		No. of Heats	Number of Tests[a]	
		Carbon Steel	Low–Alloy Steel		In Air	In Water
ANL	11–14	A106–Gr B		1	16 (1)	16 (1)
			A533–Gr B	1	16 (1)	21 (1)
GE	4–7	A516–Gr 70		1	8 (1)	14 (1)
		A333–Gr 6		1	14 (1)	
Japan	JNUFAD	A333–Gr 6		4	37 (3)	91 (3)
		A508–Cl 1		1		14 (1)
			A533–Gr B	5	106 (5)	62 (2)
			A508–Cl 2	1	28 (1)	26 (1)
			A508–Cl 3	7	195 (7)	147 (2)
MEA	8–10	A106–Gr B		1	36 (1)	18 (1)
				Total:	456	409

[a] The number within parentheses represents the number of heats used for the tests.

hourglass samples were excluded from the analysis). Some of the tests were conducted under load control (15% of the tests in air and 9% in water). The GE tests in the Dresden 1 reactor were conducted in bending with a trapezoidal waveform.

In most studies, the fatigue life of a test specimen is defined as the number of cycles for the peak tensile stress to drop 25% from its initial value. For the specimen sizes used in these studies (6 to 10–mm diameter), a 25% drop in peak tensile stress corresponds to an approximately 3–mm crack, i.e., N_{25} represents the number of cycles to initiate a 3–mm crack. The fatigue lives defined by other criteria, e.g., 50% decrease in peak tensile stress or complete failure, were normalized according to the equation

$$N_{25} = N_X / (0.947 + 0.00212\,X), \quad (1)$$

where X is the failure criteria, i.e., 25, 50, or 100% decrease in peak tensile stress. The strain rates for the tests conducted with a sine waveform were represented by average values.

METHODOLOGY

Modeling Choices

In an attempt to develop a statistical model from incomplete data and where physical processes are only partially understood, care must be taken to avoid overfit of the data. Additional terms could have been added to the statistical model and used to explain more of the current data set, i.e., to make a more powerful model. However, such changes may not hold true in other data sets, and the model would typically be less robust, i.e., it would not predict new data well. In general, complexity in the model is undesirable unless it is consistent with accepted physical processes.

Managing the tradeoff between robustness and power in the model necessarily requires application of engineering judgment. Model features that would be counter to known effects are excluded. Features that are consistent with previous studies use such results as guidance, e.g., on the boundaries and saturation points for an effect, but where there are differences from previous findings, the reasons for the differences are evaluated and an appropriate set of assumptions is incorporated into the model.

Functional Form. Different functional forms of the predictive equations (e.g., different procedures for transforming the measured variables into data used for fitting equations) were tried for several aspects of the model. Fatigue S–N data are generally expressed in terms of the Langer equation of the form

$$\varepsilon_a = B(N_{25})^{-b} + A, \quad (2a)$$

where ε_a is the applied strain amplitude and A, B, and b are parameters of the model. Equation 2a may be rearranged to express fatigue life N_{25} in terms of strain amplitude ε_a as

$$\ln(N_{25}) = [\ln B - \ln(\varepsilon_a - A)]/b. \quad (2b)$$

A function that uses an exponential transformation for strain amplitude was also tried instead of the logarithmic transformation in Eq. 2b. In the absence of well–understood physical mechanisms, either of these functional forms is acceptable and should be interpreted as a curve that happens to fit the data. The exponential form is useful for explaining the scatter of low–strain–amplitude data, while the logarithmic form is useful for explaining mid– and high–strain–amplitude data, so the choice of form must be appropriate to the range being modeled.

Grouping of Data. To estimate the parameters, the existing data were divided into three groups: air, water with modest environmental effect, and water with significant environmental effect. For each of these groups, there are natural subgroupings in which different mechanisms operate. Because the last of these groups contains relatively fewer samples than the others, a pure least–square–error model based on all data would underweight the influence of certain environmental conditions properly, and this could make the model less robust. The following method was adopted for optimizing the parameters of the model: the

nonlinear variables (strain–amplitude thresholds) were estimated from air data only, and the effects of temperature and steel type were estimated separately from air and water data. The resulting regression analysis yielded high explanatory power without sacrificing robustness across data sets.

Least–Squares Modeling within a Fixed Structure

The modeling process is iterative. First, a model is tested and optimized, and then its predictions are plotted against the actual data. By examining patterns in the residual errors of different variables or data subsets, it is possible to adjust the model; this is particularly helpful when relationships are clearly nonlinear and not well understood.

The parameters of the model are commonly established through least–squares curve–fitting of the data to either Eq. 2a or 2b. An optimization program sets the parameters so as to minimize the sum of the square of the residual errors, which are the differences between the predicted and actual values of ε_a or $\ln(N_{25})$. A predictive model based on least–squares fit on $\ln(N_{25})$ is biased for low ε_a; in particular, runoff data cannot be included. The model also leads to probability curves that converge to a single value of threshold strain. However, the model fails to address the fact that at low ε_a, most of the error in life is due to uncertainty associated with either measurement of strain or variation in threshold strain caused by material variability. On the other hand, a least–squares fit on ε_a does not work well for higher strain amplitudes. The two kinds of models are merely transformations of each other, although the precise values of the coefficients differ.

The two approaches were combined by minimizing the sum of squared cartesian distances from the data points to the predicted curve. For low ε_a, this is very close to optimizing the sum of squared errors in predicted ε_a; at high ε_a, this is very close to optimizing the sum of squared errors in predicted life; and at medium ε_a, this model combines both factors. However, because the model includes many nonlinear transformations of variables and because different variables affect different parts of the data, the actual functional form and transformations are partly responsible for minimizing the square of the errors. Functional forms and transformation are chosen a priori, and no direct computational means exist for establishing them.

To perform this optimization, it was necessary to normalize the x and y axes by assigning relative weights to be used in combining the error in life and strain amplitude. Errors in strain amplitude (%) are weighted 20 times as heavily as errors in $\ln(N_{25})$. Distance from the curve was estimated as

$$D = \left\{(x-\hat{x})^2 + \left[k(y-\hat{y})\right]^2\right\}, \tag{3}$$

where $\hat{x}$ and $\hat{y}$ represent predicted values, and k = 20. Although R–squared is only applicable for linear regression, an approximate value for combined R–squared was derived for illustrative purposes. The combined R–squared is defined as

$$1-\left(\frac{\Sigma D^2}{\Sigma Z^2}\right), \tag{4a}$$

where

$$Z = \left\{(x-x')^2 + \left[k(y-y')\right]^2\right\} \tag{4b}$$

and x' and y' represent the 25th percentile of x and y, respectively, for the sample data. The 25th percentile is selected instead of the mean because the mean values are exaggerated due to the nonlinearity of the equations, and because higher values are less influential to the model. This value is not a true R-squared, but often falls between the x–based R–squared and the y–based R–squared; it is considered to be a better qualitative measure of the model's predictive accuracy because it is not distorted in the way x–based R–squared and y–based R–squared measures would be.

Test data for heats that exhibited extreme characteristics were excluded from the analysis. Two of the 23 heats included in the data base, an A516–Gr 70 CS plate and an A508–Cl 2 alloy steel forging, show unusually high fatigue lives in air. The A516–Gr 70 steel was used by GE for the tests in the Dresden reactor. The eight tests in air show a life that is longer by nearly one order of magnitude than other CSs. These eight tests also account for nearly half of the tests at ≈250°C and tend to bias the effects of temperature on fatigue life; therefore, they were excluded from the analysis. The A508–Cl 2 steel was tested by two investigators; in strain–control mode by one investigator and in load–control mode by the other. The load–control tests in air at RT show significantly longer lives than the tests conducted in the strain–control mode. The 15 load–control tests were excluded from the analysis.

The power of the model would have been increased significantly by adding an adjustment for each heat, i.e., by conducting "lot–centered" analyses so that the average residual error for each heat would be zero. However, the model would then be applicable only for those materials for which the lot classification is known. Such information is not available in practice. It is conceivable that with more complete data sets and comprehensive data on tensile strengths of materials from different heats, product forms, and fabrication history, this would be a useful feature to include in the model.

THE MODEL

The fatigue S–N data for CSs and LASs are best represented by

$$\begin{aligned}\ln(N_{25}) = {} & (6.667 - 0.766\, I_W) \\ & - (1.687 + 0.184\, I_S)\ln(\varepsilon_a - 0.15 + 0.04\, I_S) \\ & - (0.097 - 0.382\, I_W)\, I_S - 0.00133\, T\,(1 - I_W) \\ & + 0.554\, S^*\, T^*\, O^*\, \dot{\varepsilon}^*,\end{aligned} \tag{5}$$

where:

N_{25} = the fatigue life defined as the number of cycles for the peak tensile stress to drop 25% from its initial value,

ε_a = the applied strain amplitude in %,

T = the test temperature in °C,
I_W = 1 for water and 0 for air environment,
I_S = 1 for CS and 0 for LAS,

and S^*, T^*, O^*, and $\dot{\varepsilon}^*$ are transformed sulfur content, temperature, DO, and strain rate, respectively, defined as follows:

$$\begin{aligned} S^* &= S && (0 < S < 0.015 \text{ wt.\%}) \\ S^* &= 0.015 && (S > 0.015 \text{ wt.\%}) \end{aligned} \quad (6a)$$

$$\begin{aligned} T^* &= 0 && (T < 150°C) \\ T^* &= T - 150 && (T > 150°C) \end{aligned} \quad (6b)$$

$$\begin{aligned} O^* &= 0 && (DO < 0.05 \text{ ppm}) \\ O^* &= DO && (0.05 \text{ ppm} \le DO \le 0.5 \text{ ppm}) \\ O^* &= 0.5 && (DO > 0.5 \text{ ppm}) \end{aligned} \quad (6c)$$

$$\begin{aligned} \dot{\varepsilon}^* &= 0 && (\dot{\varepsilon} > 1 \text{ \%/s}) \\ \dot{\varepsilon}^* &= \ln(\dot{\varepsilon}) && (0.001 \le \dot{\varepsilon} \le 1 \text{ \%/s}) \\ \dot{\varepsilon}^* &= \ln(0.001) && (\dot{\varepsilon} < 0.001 \text{ \%/s}) \end{aligned} \quad (6d)$$

Equation 5 is a modified version of the model presented earlier in NUREG/CR–6237 (18). The following method was adopted for optimizing the parameters of the model. The constants 0.15 or 0.11 in the second term define the threshold strain amplitude or endurance limit for LAS and CS, respectively (in % strain). These threshold values are not easily optimized with scant data at low strain amplitude, and therefore were established from earlier models and from visual inspection of the data. The coefficient in second term, intercept (first and third terms), and temperature dependence (fourth term) were then established from the air data for CS and LAS. The effect of water, including the coefficient for the fifth term, were optimized using the entire data set. A combined R–squared value of 80.1% was obtained for the analysis. The life prediction R–squared value for this model is 83.9% and the strain amplitude prediction R–squared value is 87.6%. It would have been possible to develop a model with higher R-squared by optimizing for all data points and all parameters simultaneously. Instead, the parameters were optimized in an iterative fashion in order to yield high explanatory power without sacrificing robustness across data sets.

The experimental values of fatigue life of CS and LAS in air and water and those predicted from Eq. 5 are plotted in Fig. 2. Examples of estimated and experimental fatigue S–N curves for specific data sets for CS and LAS in high–DO water re shown

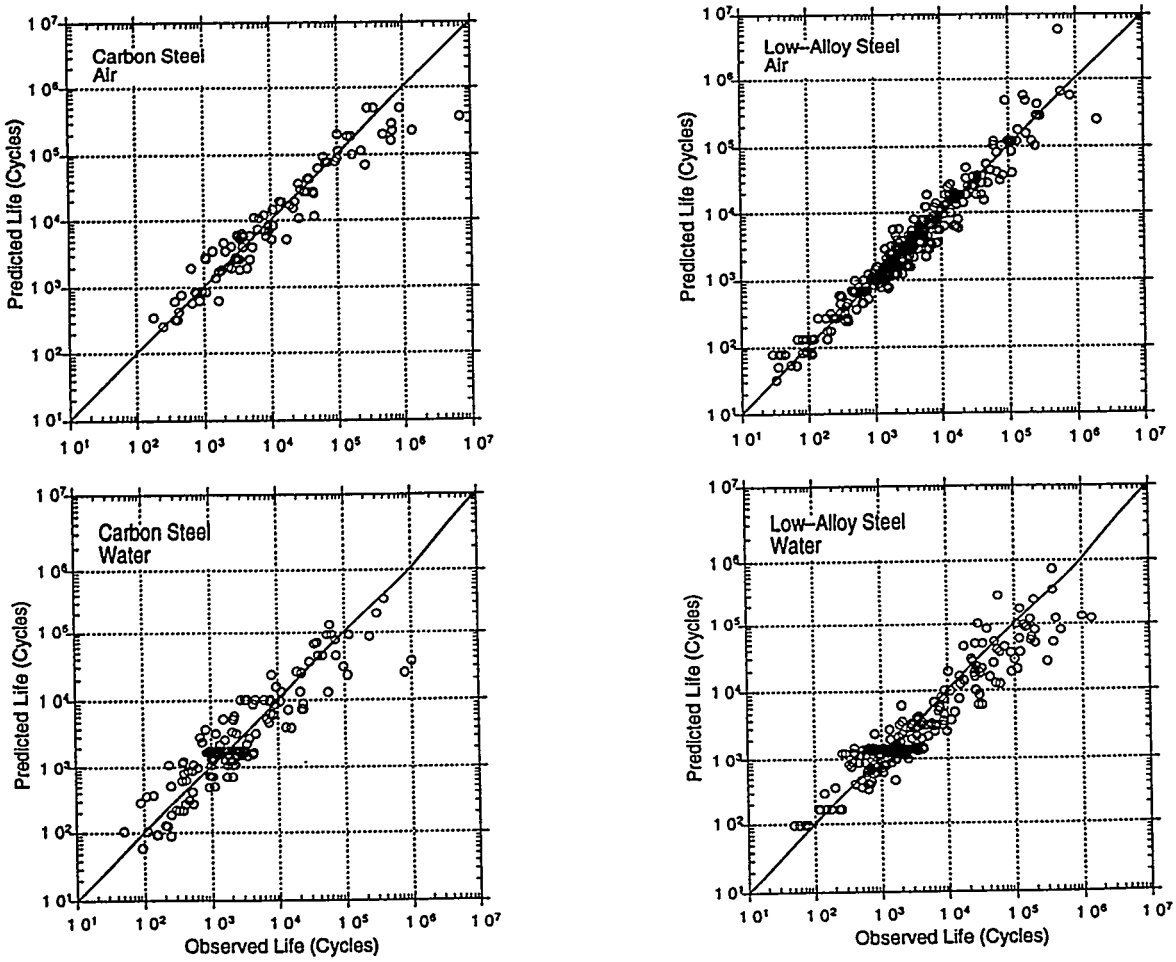

Figure 2. Experimental and predicted fatigue lives of carbon and low–alloy steels in air and water environments

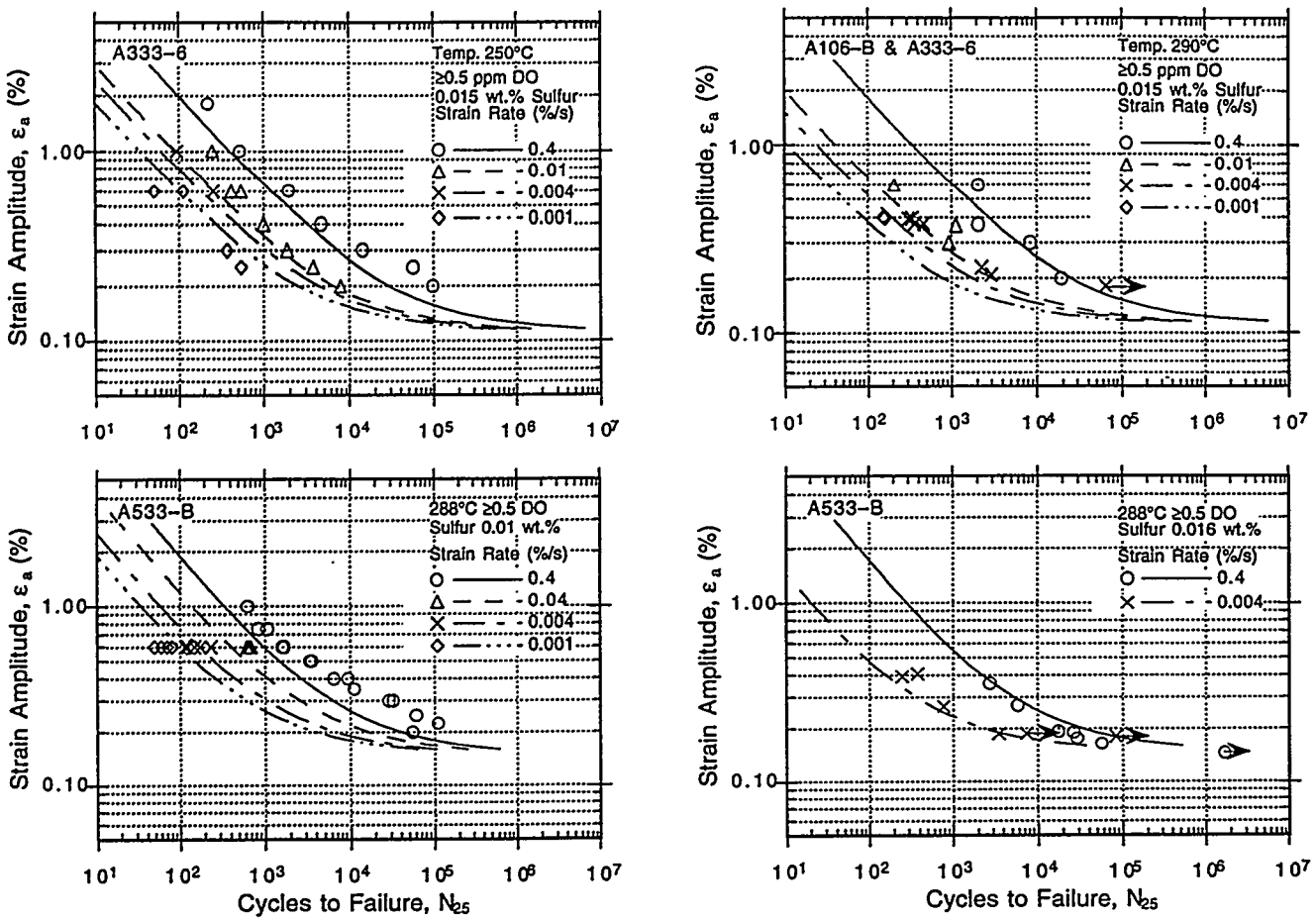

Figure 3. Fatigue S–N behavior for carbon and low–alloy steels, estimated from the model and determined experimentally in water containing ≥0.5 ppm dissolved oxygen

Table 2. Estimates of factor by which fatigue life is changed by varying a specific variable

Material or Service Variable	Change in Variable[a]		Factor by Which Fatigue Life is Changed		
	from	to	Air Env.	Water Environment[b] Moderate	Water Environment[b] Significant
Indicator I_W (LAS)	1	0	–	2.15	2.15
Indicator I_W (CS)	1	0	–	1.47	1.47
Temperature (°C)	300	25	1.44	1.0	73.6
Dissolved Oxygen (ppm)	0.50	<0.05	–	1.0	73.6
Strain Rate (%/s)	0.001	1.00	1.0	1.0	73.6
Sulfur in Steel (wt.%)	0.015	0.003	1.0	1.0	59.4

[a] The change in fatigue life is estimated by varying a specific variable from its base value to the new value while the other variables are maintained at their base values. The effect of steel type is not included because it varies with strain range.

[b] Effect of water environment is moderate when any one of the following three conditions is not satisfied: temperature ≥150°C, DO ≥0.05 ppm, and strain rate <1%/s. Environmental effects are significant when all three conditions are satisfied.

in Fig. 3. The predicted fatigue lives show good agreement with the experimental data.

The model can be used to estimate the factor by which fatigue life is changed when a specific variable is varied within the range of the experimental data base. These factors for air and water environments, determined by varying an individual variable from its base value at one end of the range to a value at the other end of the range, are given in Table 2. The factors for water environment have been divided into two columns based on whether environmental effects on fatigue life are moderate or significant. The results indicate that the effect of material and loading variables on fatigue life is insignificant in air or when environmental effects are moderate (e.g., when any one of the

following conditions is true: temperature <150°C, DO <0.05 ppm, or strain rate ≥1%/s). Under these conditions, only steel type and temperature influence fatigue life. Material and loading variables such as sulfur content in the steel, temperature, DO, and strain rate, have a large effect on fatigue life in water when all of the following conditions are true: temperature ≥150°C, DO ≥0.05 ppm, or strain rate <1%/s. Under these conditions, varying any one of the four variables, e.g., temperature, DO, sulfur content in steel, or strain rate, from their base value at one end of the range to a value at the other end of the range decreases fatigue life by a factor ≈70. The values listed in the last column of Table 2 represent the maximum change in fatigue life for the range of variables of the data base; these values will be lower for other base values of the variables. For example, the effect of strain rate will be much lower at 200 instead of 290°C or for a steel containing 0.007 instead of 0.015 wt.% sulfur.

SUMMARY STATISTICS

Statistical Significance of Parameter Values

Errors are associated with estimates of parameter values. These errors are a function of the importance and strength of the effects in question, as well as of the amount and variation of the data used to estimate them. The standard error and t–statistic for the best–fit values of the coefficients for various parameters in the model are presented in Table 3. Confidence intervals for the parameter values are based on the specific data sets used to determine them, rather than on the entire data set. The estimates of error were determined by fixing nonlinear aspects and taking the linear regression output for each data set for a model to predict $\ln(N_{25})$. These errors were then applied to the parameters obtained in the cartesian distance squared error–minimizing model; as for any nonlinear regression, the resulting confidence intervals and t–statistics are not exact. The t–statistic for each variable is the number of standard errors from 0 to the estimated value of the coefficients; it is an indication of the statistical significance of that parameter of the model. Values of t–statistic >2.5 provide convincing evidence of the statistical significance of the variable. These results are conditional on the assumptions about functional form and nonlinear or nonuniform aspects of the model; confidence in the functional form is established by the better performance of one model over another.

The 95% lower bound for the estimate of each coefficient (fifth column of Table 3) is approximately 2 standard errors below its mean estimate, and the 95% upper bound (sixth column of Table 3) is approximately 2 standard errors above the mean estimate. The 99% lower and upper bounds are approximately 2.5 standard errors from the mean estimate. The last column of Table 3 gives the factor by which predicted life would change if either the lower or upper 95% bound on the corresponding coefficient, whichever would lead to a shorter life, were assumed instead of its mean value. An example of how to interpret this table is, for CS or LAS, if the coefficient for temperature is at its mean estimated value of –0.00133, predicted life would be 1.183 times greater than if the coefficient for temperature is at its 95% lower bound value of –0.00189.

Normality Tests

Residual errors were tested to determine whether they follow a normal distribution. The errors (specifically, the cartesian distances from the predicted life and strain amplitude values) for the total data set appear, upon both visual inspection and statistical analysis, to be approximately normal; the chi–square test value for the normal distribution with 10 categories is 1.147; the Anderson-Darling value is 3.086; the Kolmogorov-Smirnoff value is 0.031. Errors in the prediction of $\ln(N_{25})$ are not normally distributed because of large errors for low strain. Errors in the prediction of strain amplitude are also not normally distributed because of large errors for short–lived specimens. For strain amplitudes >0.24, errors in prediction of $\ln(N_{25})$ are close to normal (skewness = 0.04, kurtosis = 3.32, compared to 0 and 3, respectively, for a normal distribution), and for specimens with fatigue lives >1000 cycles, errors are approximately normal but more peaked (skewness = 0.015, kurtosis = 5.95). On visual inspection, both sets of errors appear to be close to normally distributed and reasonably behaved at the extremes.

A more precise characterization of the residuals may be derived by examining subsets of the data that are expected to follow different distributions. The existing data in these smaller groups are inadequate to make statements about the exact generating distribution with any confidence.

Table 3. Standard error and t–statistic for the coefficients of various parameters in the model

Variable	Coefficient	Standard Error	t–Statistic	Lower 95%	Upper 95%	Factor
Intercept (LAS)	6.667	0.0578	115.3	6.552	6.782	1.122
Intercept (CS)	6.570	0.0933	70.4	6.385	6.755	1.203
Intercept (LAS Water)	–0.766	0.0700	–10.9	–0.905	–0.627	1.149
Intercept (CS Water)	-0.384	0.1130	–3.4	–0.608	–0.160	1.251
Strain Amplitude (LAS)	–1.687	0.0218	–77.5	–1.733	–1.647	1.042
Strain Amplitude (CS)	–1.871	0.0407	–45.9	–1.951	–1.789	1.084
Environmental Effect	0.554	0.0350	15.8	0.485	0.623	1.708
Temperature	–0.00133	0.00028	–4.75	–0.00189	–0.00077	1.183

PROBABILITY DISTRIBUTIONS OF FATIGUE LIFE

The average distance of data points from the mean curve does not vary much across different environmental conditions, except for steel type. However, the error in predicted life tends to be greater at low ε_a. To develop a probability distribution on life, we start with the assumption that there are two sources of prediction error, viz., error in the estimated difference between strain amplitude and threshold (including both measurement error and material variability that leads to variation in the threshold value) and scatter in fatigue life due to uncertainty in test and material conditions or other unexplained variation.

In the limit, the standard deviation of distance from the mean curve at low strain amplitudes is equal to the standard deviation of the measurement error times the weighting factor of 20. At high strain amplitudes, the standard deviation of distance from the mean curve is equal to the standard deviation of the scatter error. The corresponding standard deviation of distance from the mean S–N curve is 0.518 for life N_{25} and 0.0259 for ε_a. The xth percentile of the probability distribution on life is given by

$$\ln(N_{25}) = (6.667 - 0.766\, I_W) - (1.687 + 0.184\, I_S) \ln(\varepsilon_a - 0.15 + 0.04\, I_S + 0.0259\, F^{-1}[1-x]) - (0.097 - 0.382\, I_W)\, I_S - 0.00133\, T\,(1 - I_W) + 0.554\, S^*\, T^*\, O^*\, \dot{\varepsilon}^* + 0.518\, F^{-1}[x]]), \quad (7)$$

where $F^{-1}[x]$ is the inverse of the standard normal cumulative distribuition function. This technique leads to probability curves that are farther from the mean curve (by a factor of up to 1.4) in the middle range of strain amplitudes (i.e., for ε_a=0.2–0.4%) than at low and high strain amplitudes. For example, the xth percentile probability curve implies a greater average squared distance from the mean curve than the distance actually derived from the data. An examination of the residual errors is consistent with this shape of curve, but it is not clear whether the technique overestimates uncertainty in the middle while being unbiased at the extremes, or has a slight bias for the entire range of strain amplitudes. Other less–conservative techniques that could be used instead would be to assume constant distances between probability curves and the mean curve (this approach is more computationally complex), or to apply a factor of 0.8 to the standard deviations for ε_a or $\ln(N_{25})$. With additional data, it might be possible to choose one of these less–conservative techniques.

The estimated probability curves for the fatigue life of CS and LAS in air and simulated PWR water are shown in Figs. 4 and 5, respectively. They appear to be consistent with the experimental data; nearly all of the experimental data are bounded by the 5% probability curve. The results indicate that at high strain amplitudes (e.g., >0.3%) the 5% probability curve is a factor of

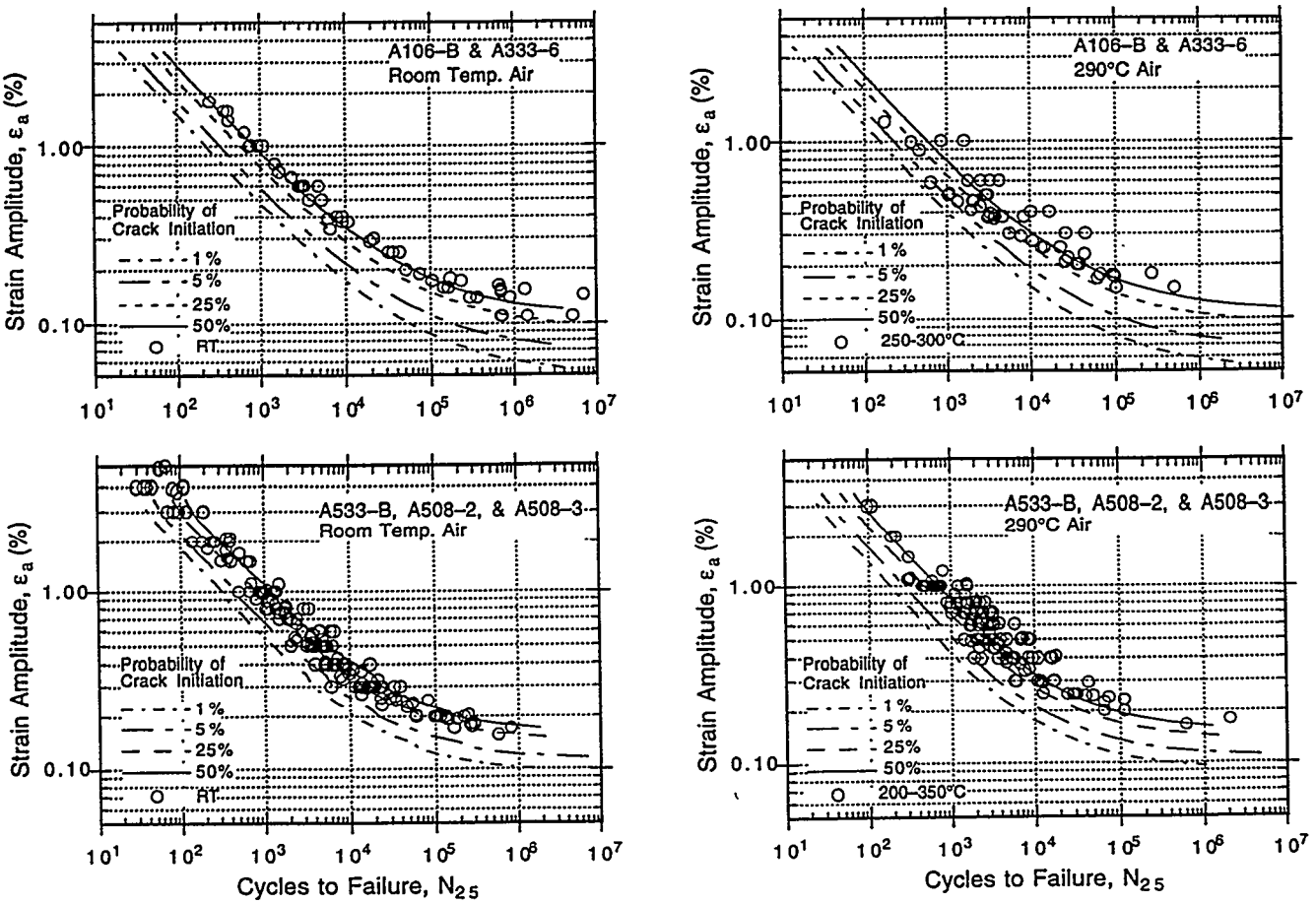

Figure 4. Probability of fatigue crack initiation in carbon and low–alloy steels in air at room temperature and 290°

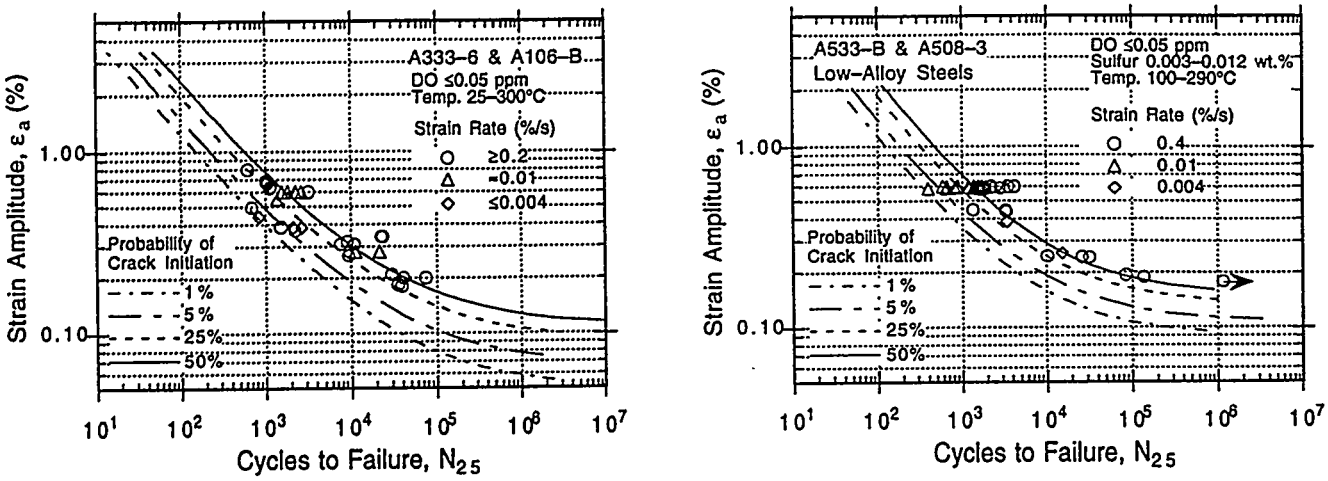

Figure 5. Probability of fatigue crack initiation in carbon and low–alloy steels in simulated PWR environment

≈2.5 lower in life than the mean curve (50% probability) and 1% probability curve is ≈3.7 lower. At low strain amplitudes (e.g., <0.2%), the 5% probability curve for CS is a factor of ≈1.7 lower in strain amplitude than the mean curve and 1% probability is ≈2.2 lower. The corresponding factors for 5 and 1% probability curves for LAS are ≈1.4 and 1.7, respectively.

FATIGUE S–N BEHAVIOR OF COMPONENTS

Several variables can influence fatigue life; these can be broadly classified into three groups:

1. Material
   a. Composition: sulfur content
   b. Metallurgy: grain size, inclusions, orientation within a forging or plate
   c. Processing: cold work, heat treatment
   d. Size and geometry
   e. Surface finish: fabrication surface condition
   f. Surface preparation: surface work hardening
2. Loading
   a. Strain rate: rise time
   b. History: linear damage summation or Miner's rule
   c. Mean stress
   d. Biaxial effects: constraints
3. Environment
   a. Water chemistry: DO, lithium hydroxide, boric acid concentrations
   b. Temperature
   c. Flow rate

The existing fatigue S–N data base covers an adequate range of material parameters (a–c), a loading parameter (a), and environment parameters (a and b); therefore, the effects of these parameters have been incorporated into the model. Loading parameters (b–d) are covered by design procedures and need not be considered in the S–N curves.

The existing data are conservative with respect to the effects of surface preparation because the fatigue S–N data are obtained for specimens that are free of surface cold work, which typically gives longer fatigue lives. Fabrication procedures for fatigue test specimens generally follow ASTM guidelines which require that the final polishing of the specimens should avoid surface work hardening. The existing data are inadequate to evaluate the contributions of flow rate on fatigue life; most of the tests in water have been conducted at relatively low flow rates. Consequently, only the contributions of size, geometry, and surface finish need to be considered in development of fatigue crack–initiation curves that are applicable to components.

Effect of Size and Geometry

The effect of specimen size on the fatigue life of CS and LAS has been investigated for smooth specimens of various diameters in the range of 2–60 mm (20–23). No intrinsic size effect has been observed for smooth specimens tested in axial loading or plain bending. However, a size effect does occur in specimens tested in rotating bending; fatigue endurance limit decreases by ≈25% by increasing the specimen size from 2 to 16 mm but does not decrease further for larger sizes (23). In addition, some effect of size and geometry has been observed on small–scale vessel tests conducted at Ecole Polytechnique in conjunction with the full–size pressure vessel tests carried out by Southwest Research Institute (24). The tests at the Ecole Polytechnique were conducted in RT water on ≈305–mm inner diameter, 19–mm–thick shells with nozzles made by machining bar stock. The results indicate that the number of cycles to form an 3–mm crack in an 19–mm–thick shell may be 30–50% lower than those in a small test specimen (18). Thus, a factor of ≈1.4 on cycles and a factor of ≈1.25 on strain can be used to account for size and geometry.

Effect of Surface Finish

Fatigue life is sensitive to surface finish; cracks can initiate at surface irregularities that are normal to the stress axis. The

height, spacing, shape, and distribution of surface irregularities are important for crack initiation. The most common measure of roughness of surfaces is average roughness R_a, which is a measure of the height of the irregularities. In addition, a wavelength parameter is used to characterize the spacing of the peaks and valleys of the surface, and a skewness parameter is a measure of the symmetry of the profile about the mean line.

Information is very limited on detailed characterization of surfaces in terms of height, shape, and distribution of surface irregularities produced by different manufacturing and fabrication processes. Typical values of average roughness for surfaces finished by different metalworking processes in the automotive industry (data from Ref. 25) are given in Table 4. Limited data on surface height distributions for mild steel surfaces finished by centerless grinding show a normal distribution, whereas surfaces finished by other methods are more peaked or asymmetrical than a normal distribution (26). For the level of precision in the present model and in the functional relationship between surface roughness and fatigue life given below, the exact distribution should not matter beyond the mean and variance.

Table 4. Typical average roughness values for surfaces finished by various processes

Process	R_a (mm)
Planing, shaping	1 – 25
Milling	1 – 6
Drawing, extrusion	1 – 3
Turning, boring	0.4 – 6
Grinding	0.1 – 2
Honing	0.1 – 1
Polishing	0.1 – 0.4
Lapping	0.05 – 0.4
Cast	0.9 – 72

Investigations of the effects of surface roughness on the low–cycle fatigue of Type 304 stainless steel in air at 593°C indicate that fatigue life decreases as surface roughness increases (27,28). The effect of roughness on crack initiation $N_i(R)$ is given by

$$N_i(R_q) = 1012\, R_q^{-0.21}, \qquad (8)$$

where the RMS value of surface roughness R_q is in μm. A study of the effect of surface finish on fatigue life of CS in RT air, showed a factor of 2 decrease in life when R_a is increased from 0.3 to 5.3 μm (29). These results are consistent with Eq. 8.

Table 4 shows that an R_a of 3 μm (or R_q of 4 μm) represents the maximum surface roughness for drawing/extrusion, grinding, honing, and polishing processes and mean value for the roughness range for milling and turning processes. For CS or LAS, an R_q of 4 μm in Eq. 8 (R_q of a smooth polished specimen is ≈0.0075 μm) would decease fatigue life by a factor of ≈3 (27). No information on the effect of surface finish on endurance limit of CSs and LASs is available. It may be approximated as a factor of ≈1.3 on strain (The factor applied on strain (K_S) is obtained from the factor applied on cycles (K_N) by using the relationship $K_S=(K_N)^{0.2326}$).

Estimated Fatigue S–N Curves for Components

The discussions presented above indicate that uncertainties associated with component size/geometry and surface finish can be accounted for by lowering the best–fit or mean curve for smooth test specimens by factors of 1.4 and 3, respectively, on cycles and by 1.25 and 1.3, respectively, on strain. The probability distribution curves presented in the previous section indicate that relative to the mean curve (50% probability), the 5% probability for fatigue cracking in smooth test specimens is lower by a factor of 2.5 on cycles and 1.7 on strain. The factors on strain primarily account for the variation in threshold strain (i.e., fatigue endurance of the material) caused by either material variability, component size, or surface finish. The effect of these parameters on threshold strain should not be cumulative but rather would be controlled by the parameter that has the largest effect, e.g., a factor of 1.7 on strain (largest of 1.25, 1.3, and 1.7) is adequate to account for the uncertainties due to material variability, size/geometry, and surface finish. Consequently, the fatigue S–N curves for components can be obtained by lowering the probability distribution curves for smooth test specimens by a factor of 4 (i.e., product of 1.4 and 3) on cycles to include the effects of size/geometry and surface finish. The contributions of material variability have been incorporated into the statistical model and probability distribution curves.

Fatigue S–N curves that represents 1, 5, 25, and 50% probability of crack initiation in CS and LAS components in RT water are shown in Fig. 6. The curves were obtained by lowering the probability distribution curves for smooth test specimens by a factor of 4 on cycles to account for the uncertainties due to component size/ geometry and surface finish. The results of full–size–vessel tests (24), in terms of cycles to initiate a crack, are also plotted in the figure. For both steels, the estimated curves are consistent with the test results; the test data are bounded by the 5% probability curve.

The probabilities of fatigue cracking in CS or LAS components in air at RT and 290°C are compared with the current ASME Code design curve in Fig. 7. The probability curves were also adjusted for the effect of mean stress by using the modified Goodman relation

$$S_a' = S_a\left(\frac{\sigma_u - \sigma_y}{\sigma_u - S_a}\right) \qquad \text{for } S_a < \sigma_y, \qquad (9)$$

where S_a is the applied stress amplitude (expressed as the product of elastic modulus E and ε_a), S_a' is the adjusted value of stress amplitude, and σ_y and σ_u are yield and ultimate strengths of the material, respectively. The mean stress adjust-

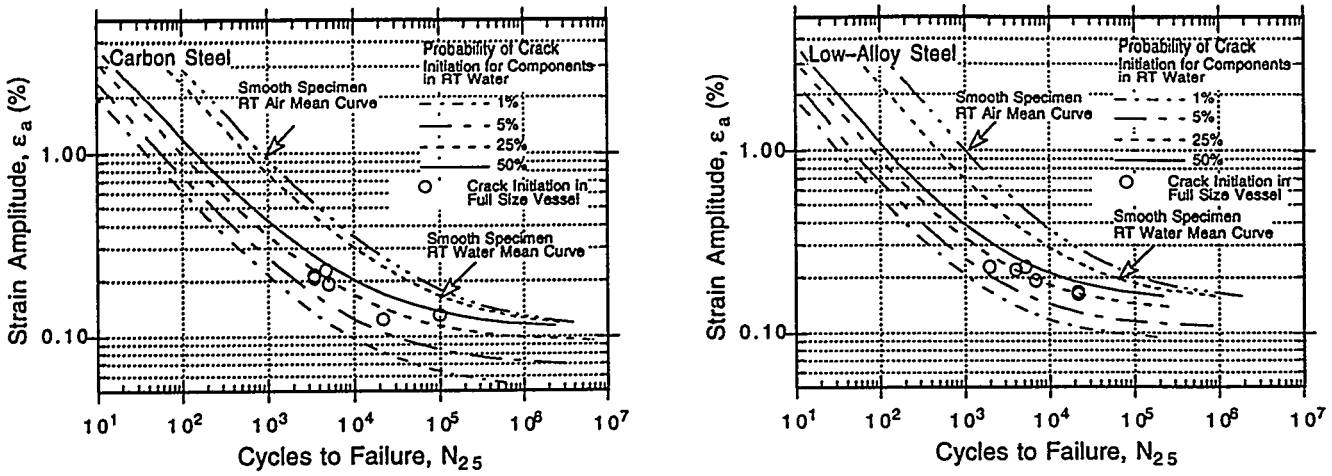

Figure 6. Probability of fatigue cracking in carbon and low–alloy steels in room–temperature water

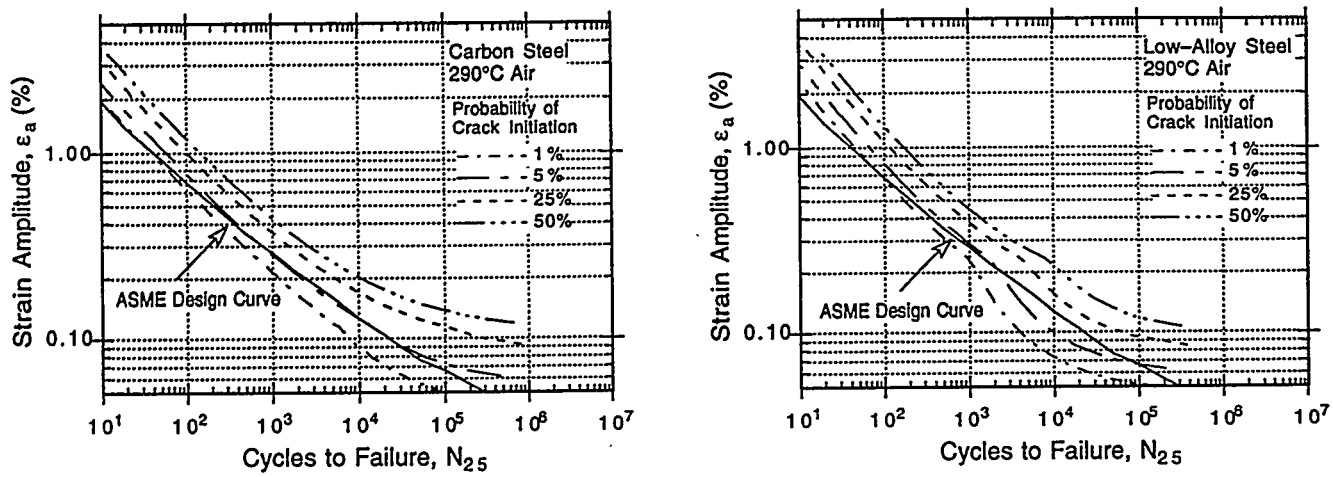

Figure 7. Probability of fatigue cracking in carbon and low–alloy steels in air at 288°C

ment is larger for LASs than for CSs because of their high yield strength. The estimated probability curves indicate that the ASME Code design curve corresponds to ≈5% probability of fatigue cracking in CSs or LASs. The fatigue strain vs. life curves shown in Fig. 7 may be expressed as stress vs. life by multiplying the strain values by the appropriate elastic modulus, i.e., $S_a = E\,\varepsilon_a$.

The probability of fatigue cracking in CSs in PWR environment at 290°C and in high–DO water at 200 and 250°C are shown in Figs. 8 and 9, respectively. The NUREG/CR–5999 interim design curves (17) and the ASME Code design curve are also included in the figures. The results indicate that in PWR environments, the Code design curve corresponds to a ≈5% probability of fatigue cracking, and the proposed interim design curve represents a 1% or lower probability. The current ASME Code fatigue design curve for CSs and LASs does not adequately address the effect of environment on fatigue life in high–DO water. For service conditions that yield maximum effect of environment on fatigue life, e.g., ≥0.5 ppm DO, ≥0.015 wt.% S, ≤0.001%/s strain rate, and >150°C, the estimated 5% probability curves are a factor of ≈5 lower at 200°C and a factor of ≈20 lower at 250°C than the current ASME Code design curve. Under these conditions, the proposed interim design curves represent <1% probability of fatigue cracking at 200°C and 1–5% probability at 250°C.

CONCLUSIONS

The existing fatigue strain vs. life (S–N) data from the United States and Japan for CSs and LASs used in the construction of nuclear power plant components have been compiled and categorized according to material, loading, and environmental conditions. A statistical model has been developed for estimating the effects of the various test conditions on fatigue life. In this paper, experimental fatigue S–N data are considered to represent the number of cycles required to initiate a 3–mm surface crack in a smooth specimen. The results of the analysis have been used to estimate the probability of initiating fatigue cracks in smooth specimens. Fatigue S–N curves for components can be deter-

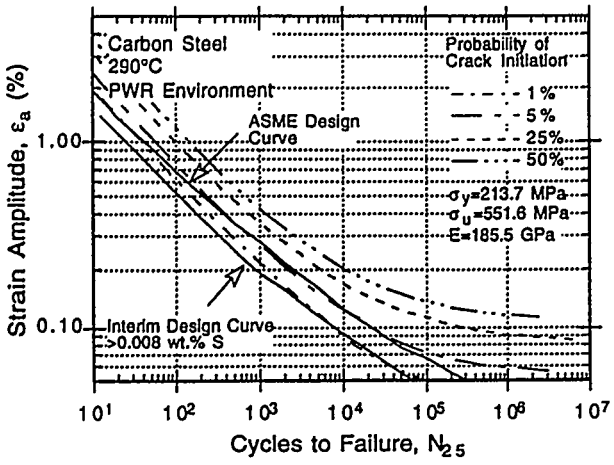

Figure 8. Probability of fatigue cracking in carbon steel in PWR environment, the proposed interim design curve for carbon steel in water with <0.1 ppm DO, and the ASME design curve

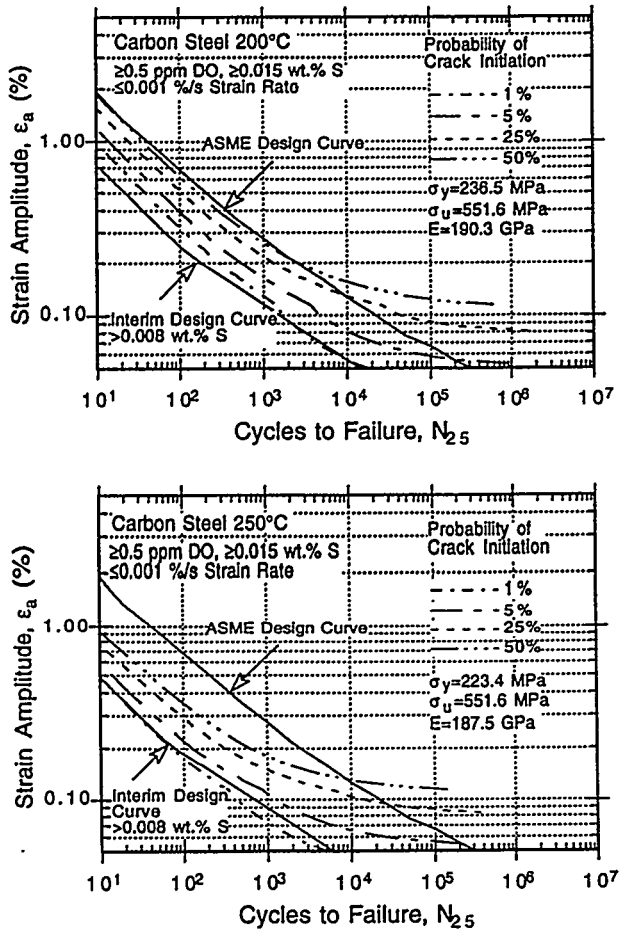

Figure 9. Probability of fatigue cracking in carbon steel at 200 and 250°C in high–DO water, the proposed interim design curve for carbon steel in water with >0.1 ppm DO, and the ASME design curve

mined by setting margins for size, geometry, and surface finish to the crack initiation curves estimated from the model. Data available in the literature were reviewed to evaluate the effects of size, geometry, and surface finish of a component on its fatigue life. The data indicate that a factor of 1.4 may be used to account for size and geometry and a factor of 3 to account for surface roughness.

The fatigue S–N curves for components were obtained by lowering the probability distribution curves for smooth test specimens by a factor of 4 (i.e., the product of 1.4 and 3) on cycles to account for the uncertainties due to size/geometry and surface finish. The results indicate that in either air or PWR water environments at 290°C, the ASME Code design curve represents an ≈5% probability of fatigue cracking in CS or LAS components. The current ASME Code fatigue design curve for carbon and low–alloy steels does not adequately address the effect of environment on fatigue life in high–DO water. For service conditions that yield maximum effect of environment on fatigue life, e.g., ≥0.5 ppm DO, ≥0.015 wt.% S, ≤0.001%/s strain rate, and >250°C, the estimated 5% probability curves are more than a factor of 20 lower than the current ASME Code design curve.

ACKNOWLEDGMENTS

This work was supported by the Engineering Issues Branch, Office of Nuclear Regulatory Research (RES), U.S. Nuclear Regulatory Commission (NRC), under FIN Number W6077–3; Project Manager: Craig Hrabal. The authors thank Bill Shack and Ron Whitfield for their helpful discussions.

REFERENCES

1. "ASME Boiler and Pressure Vessel Code Section III – Rules for Construction of Nuclear Power Plant Components," The American Society of Mechanical Engineers, 345 East 47th Street, New York, NY 10017.
2. "Criteria of Section III of the ASME Boiler and Pressure Vessel Code for Nuclear Vessels," The American Society of Mechanical Engineers, United Engineering Center, New York, Library of Congress Catalog No. 56–3934, 1989.
3. "Tentative Structural Design Basis for Reactor Pressure Vessels and Directly Associated Components (Pressurized, Water Cooled Systems)," PB 151987, U.S. Dept. of Commerce, Office of Technical Service, 1 Dec. 1958 Revision.
4. Hale, D. A., Wilson, S. A., Kiss, E., and Gianuzzi, A. J., "Low Cycle Fatigue Evaluation of Primary Piping Materials in a BWR Environment," GEAP–20244, U.S. Nuclear Regulatory Commission, Sept. 1977.
5. Hale, D. A., Wilson, S. A., Kass, J. N., and Kiss, E., "Low Cycle Fatigue Behavior of Commercial Piping Materials in a BWR Environment," *J. Eng. Mater. Technol.*, Vol. 103, pp. 15–25, 1981.

6. Ranganath, S., Kass, J. N., and Heald, J. D., "Fatigue Behavior of Carbon Steel Components in High–Temperature Water Environments," in *Low–Cycle Fatigue and Life Prediction*, ASTM STP 770, C. Amzallag, B. N. Leis, and P. Rabbe, eds., American Society for Testing and Materials, Philadelphia, PA, pp. 436–459, 1982.

7. Ranganath, S., Kass, J. N., and Heald, J. D., "Fatigue Behavior of Carbon Steel Components in High–Temperature Water Environments," in *BWR Environmental Cracking Margins for Carbon Steel Piping*, EPRI NP–2406, Electric Power Reasearch Institute, Palo Alto, CA, Appendix 3, May 1982.

8. Terrell, J. B., "Fatigue Life Characterization of Smooth and Notched Piping Steel Specimens in 288°C Air Environments," NUREG/CR–5013, MEA–2232, May 1988.

9. Terrell, J. B., "Fatigue Strength of Smooth and Notched Specimens of ASME SA 106–B Steel in PWR Environments," NUREG/CR–5136, MEA–2289, Sept. 1988.

10. Terrell, J. B., "Effect of Cyclic Frequency on the Fatigue Life of ASME SA–106–B Piping Steel in PWR Environments," *J. Mater. Eng.*, Vol. 10, pp. 193–203, 1988.

11. Hicks, P. D., "Fatigue of Ferritic Steels," in *Environmentally Assisted Cracking in Light Water Reactors: Semiannual Report October 1990—March 1991*, NUREG/CR–4667 Vol. 12, ANL–91/24, pp. 3–18, Aug. 1991.

12. Hicks, P. D., and Shack, W. J., "Fatigue of Ferritic Steels," in *Environmentally Assisted Cracking in Light Water Reactors, Semiannual Report, April–September 1991*, NUREG/CR–4667 Vol. 13, ANL–92/6, pp. 3–8, March 1992.

13. Chopra, O. K., Michaud, W. F., and Shack, W. J., "Fatigue of Ferritic Steels," in *Environmentally Assisted Cracking in Light Water Reactors, Semiannual Report, October 1992–March 1993*, NUREG/CR–4667 Vol. 16, ANL–93/27, pp. 3–19, Sept. 1993.

14. Chopra, O. K., Michaud, W. F., Shack, W. J.,and Soppet, W. K., "Fatigue of Ferritic Steels," in *Environmentally Assisted Cracking in Light Water Reactors, Semiannual Report, April–September 1993*, NUREG/CR–4667 Vol. 17, ANL–94/16, pp. 3–19, June 1994.

15. Higuchi, M., and Iida, K., "Fatigue Strength Correction Factors for Carbon and Low–Alloy Steels in Oxygen–Containing High–Temperature Water," *Nucl. Eng. Des.* **129**, pp. 293–306, 1991.

16. K. Iida, H. Kobayashi, and M. Higuchi, "Predictive Method of Low Cycle Fatigue Life of Carbon and Low Alloy Steels in High Temperature Water Environments," NUREG/CP–0067, MEA–2090, Vol. 2, April 1986.

17. Majumdar, S., Chopra, O. K., and Shack, W. J., "Interim Fatigue Design Curves for Carbon, Low–Alloy, and Austenitic Stainless Steels in LWR Environments," NUREG/CR–5999, ANL–93/3, April 1993.

18. Keisler, J., Chopra, O. K., and Shack, W. J., "Statistical Analysis of Fatigue Strain–Life Data for Carbon and Low–Alloy Steels," NUREG/CR–6237, ANL–94/21, Aug. 1994.

19. James, B. A., Paul, L. D., and Miglin, M. T., "Low Cycle Fatigue Crack Initiation in SA–210 A1 Carbon Steel Boiler Tubing in Contaminated Boiler Water," in *Fatigue, Degradation and Fracture*, PVP–Vol. 195, W. H. Bamford, C. Becht, S. B. Bhandari, J. D. Gilman, L. A. James, and M. Prager, eds., American Society of Mechanical Engineers, New York, pp. 13–19, 1990.

20. Peterson, R. E., "Fatigue Tests of Small Specimens with Particular Reference to Size Effect," *Trans. Amer. Soc. Steel Testing* **18**, 1041–1053, 1930.

21. Morkovin, D., and Moore, H. F., "Third Progress Report on the Effect of Size of Specimen on Fatigue Strength of Three Types of Steel," *Proc. Amer. Soc. Test. Mater.* **44**, 137–158, 1944.

22. Philips, C. E., and Heywood, R. B., "The Size Effect in Fatigue of Plain and Notched Steel Specimens Loaded Under Reversed Direct Stress," *Proc. Inst. Mech. Engr.* **165**, 113–124, 1951.

23. Massonnet, C., "The Effect of Size, Shape, and Grain Size on the Fatigue Strength of Medium Carbon Steel," *Proc. Amer. Soc. Test. Mater.* **56**, 954–978, 1956.

24. Kooistra, L. F., Lange, E. A., and Pickett, A. G., "Full–Size Pressure Vessel Testing and Its Application to Design," *J. Eng. Power*, **86**, 419–428, 1964.

25. Stout, K. J., "Surface Roughness – Measurement, Interpretation, and Significance of Data," *Mater. Eng.* **2**, 287–295, 1981.

26. Watson, W., King, T. G., Spedding, T. A., and Stout, K. J., "The Machined Surface – Time Series Modelling," *Wear* **57**, 195–205, 1979.

27. Maiya, P. S., and Busch, D. E., "Effect of Surface Roughness on Low–Cycle Fatigue Behavior of Type 304 Stainless Steel," *Met. Trans.* **6A**, 1761–1766, 1975.

28. Maiya, P. S., "Effect of Surface Roughness and Strain Range on Low–Cycle Fatigue Behavior of Type 304 Stainless Steel," *Scripta Metall.* **9**, 1277–1282, 1975.

29. Iida, K., "A Study of Surface Finish Effect Factor in ASME B & PV Code Section III," in *Pressure Vessel Technology* Vol. 2, L. Cengdian and R. W. Nichols, eds., Pergamon Press, New York, pp. 727–734, 1989.